

Effects of Isoxazole Herbicides on Protoporphyrinogen Oxidase and Porphyrin Physiology

Franck E. Dayan,^{†,‡} Stephen O. Duke,^{*,†,‡} Krishna N. Reddy,[†] Bruce C. Hamper,[§] and Kindrick L. Leschinsky[§]

Southern Weed Science Laboratory, Agricultural Research Service, U.S. Department of Agriculture, P.O. Box 350, Stoneville, Mississippi 38776, and Monsanto Company, 800 North Lindbergh Boulevard, St. Louis, Missouri 63167

The biochemical and physiological effects of 10 isoxazoles were investigated. The amount of protoporphyrin IX caused to accumulate by the compounds correlated well with their herbicidal activity. Protoporphyrinogen oxidase (Protox) was inhibited competitively in the proximity of the catalytic site. However, the Protox I_{50} values of the methyl esters and acid chloride derivatives were lower than expected on the basis of their *in vivo* herbicidal activity. The results suggest that some tolerance mechanism, other than differential absorption and translocation, may protect the plants against these compounds. The molecular properties of 9 isoxazoles and 2 other well-known inhibitors of different herbicide groups were compared to those of protoporphyrinogen (Protox). The most active compounds have similar bulk, electronic, and energy properties that approximate half of the Protox molecule. Furthermore, these compounds have atoms/groups on the ring that generate distinct negative electrostatic potential fields that may mimic the reactive part of the Protox molecule.

Keywords: *Isoxazolecarboxamide; peroxidizing herbicides; protoporphyrinogen oxidase; protoporphyrin IX*

INTRODUCTION

Protoporphyrinogen oxidase (Protox), the last common enzyme in the biosynthesis of heme and chlorophylls (Beale and Weinstein, 1990), is the molecular target of a large number of herbicides (Matringe et al., 1989a,b; Witkowski and Halling, 1989; Duke et al., 1990, 1991; Camadro et al., 1991; Nandihalli and Duke, 1993; Scalla and Matringe, 1994; Reddy et al., 1995). These herbicides compete with protoporphyrinogen (Protox) at or near the catalytic site on Protox (Matringe et al., 1989, 1992; Witkowski and Halling, 1989; Duke et al., 1990, 1991; Scalla et al., 1990; Varsano et al., 1990; Camadro et al., 1991; Nandihalli et al., 1992a; Nandihalli and Duke, 1993; Scalla and Matringe, 1994; Lee et al., 1995). The uniqueness and complexity of the mode of action of Protox inhibitors is illustrated in the accumulation of protoporphyrin IX (Proto IX), the catalytic product of Protox activity, occurring subsequently to inhibition of the enzyme (Matringe and Scalla, 1988; Becerril and Duke, 1989a; Matsumoto and Duke, 1990; Sherman et al., 1991a; Kojima et al., 1991). Upon inhibition of Protox, Protox, the colorless tetrapyrrole substrate of the enzyme, leaks out of the plastid (Jacobs and Jacobs, 1993) and is rapidly oxidized to Proto IX by the recently discovered plasma membrane-bound, herbicide-resistant Protox (Jacobs et al., 1991; Jacobs and Jacobs, 1993; Lee et al., 1993; Lee and Duke, 1994; Duke et al., 1994). Highly reactive singlet oxygen, generated by light activation of the photodynamic tetrapyrrole Proto IX,

is responsible for rapid membrane peroxidation and cellular death (Duke et al., 1990, 1991; Scalla et al., 1990). Strong correlations have been reported between Protox inhibition, level of Proto IX accumulation, and resulting herbicidal damage caused by several groups of Protox inhibitors (Becerril and Duke, 1989b; Sherman et al., 1991a,b; Nandihalli et al., 1992b, 1994; Watanabe et al., 1992).

A new group of herbicides, carboxylate- and haloalkyl-substituted isoxazoles (Hamper et al., 1995), with all of the structural prerequisites of Protox inhibitors (Nandihalli and Duke, 1993, 1994; Reddy et al., 1995), has recently been disclosed. Unlike most photobleaching herbicides, isoxazoles generally have more herbicidal activity when applied preemergence than postemergence (Hamper et al., 1995).

Hamper et al. (1995) reported that the 5-position of the isoxazole ring had the most pronounced effect on the activity of these compounds, with CF_2Cl and CF_3 providing greatest activity. Our study focused on the biochemical and physiological properties of the CF_2Cl perhaloalkyl group of isoxazole herbicides (Table 1). We demonstrate that most of these compounds competitively inhibit Protox. However, for some of them, there was a poor correlation between herbicidal activity at the whole plant level and their ability to inhibit Protox. We also present relationships between Proto IX accumulation and cellular leakage of these compounds and their molecular properties.

MATERIALS AND METHODS

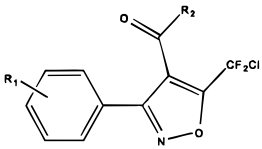
Plant Materials. For whole plant studies, seeds of morningglory (*Ipomoea* spp.), velvetleaf (*Abutilon theophrasti* Medik.), and barnyardgrass (*Echinochloa crus-galli* L.) were grown in aluminum trays containing a topsoil mixture. Plants were maintained in a greenhouse and watered daily. For the other studies, seeds of barley (*Hordeum vulgare* L. var. Morex) were germinated in flats in a commercial greenhouse substrate

* Author to whom correspondence should be addressed [fax (601) 232-1035; e-mail sduke@ag.gov].

[†] U.S. Department of Agriculture.

[‡] Present address: USDA, ARS, NPURU, P.O. Box 8048, Natural Products Center, School of Pharmacy, University of Mississippi, University, MS 38766.

[§] Monsanto Co.

Table 1. Structures and Herbicidal Activities of 10 Isoxazole Compounds


compd ^a	R ₁	R ₂	whole plants ^b	leaf disks ^c
1	4-CF ₃	OMe	—	—
2	4-Cl	OMe	++	+
3	4-Cl	OH	—	—
4	4-Cl	Cl	—	+
5	4-Cl	NH ₂	++	++
6	4-Br	NH ₂	++	+
7	2-F, 4-Cl, 5-propargyl	NH ₂	+++	+++
8	2-F, 4-Cl	(<i>RS</i>)-NHCH(CH ₃)COOEt	?	++
9	2-F, 4-Cl	(<i>R</i>)-NHCH(CH ₃)COOEt	++	+++
10	2-F, 4-Cl	(<i>S</i>)-NHCH(CH ₃)COOEt	+	—

^a Compounds 1–4, acid, ester, and acid chloride series; 5–7, carboxamide series; 8–10, amino series. ^b Based on GR₈₀ preemergence activity on morningglory, velvetleaf, and barnyardgrass; — = >5.6 kg ha⁻¹; + = 1.1–5.6 kg ha⁻¹; ++ = 0.1–1.1 kg ha⁻¹; +++ = <0.1 kg ha⁻¹. ^c Based on leaf disk assays for electrolyte leakage; — = no leakage; + = slight leakage; ++ = moderate leakage.

(Jiffy-Mix; JPA, West Chicago, IL) and watered with distilled water. Plants were grown at 25 °C under white light of 500 μmol m⁻² s⁻¹ photosynthetically active radiation (PAR) and >90% relative humidity. Some barley plants were grown under similar conditions but in darkness.

Herbicidal Activity. For the electrolyte leakage experiment, leaf tissues were sectioned from 7-day-old light-grown plants as before (Kenyon et al., 1985) and were treated with the isoxazole compounds depicted in Table 1 (technical grade >96% purity) at 10 μM. All compounds were dissolved in methanol except compounds 4–7, which were dissolved in acetone either because of low methanol solubility (carboxamides, 5–7) or because of instability in methanol (acid chloride, 4). Controls contained the same amount of methanol or acetone without the test compounds. The final concentration of methanol or acetone in the dishes was 1% (v/v). The tissues were incubated at 25 °C in darkness for 20 h and then exposed to 500 μmol m⁻² s⁻¹ PAR.

In whole plant studies, plants were sprayed with technical grade material in a 50:50 acetone/water solution. The preemergence application rates ranged from 0.004 to 11.2 kg ha⁻¹. These applications were made in a spray chamber, utilizing an 8001E nozzle and a spray pressure of 170 kPa. The trays were placed on a greenhouse bench where 0.64 cm of overhead irrigation was applied. Subsequent watering was applied by subirrigation. Herbicidal activity was evaluated approximately 10–14 days after seeding and treatment. Herbicidal activity was expressed as a GR₈₀ (kg ha⁻¹) for each species, which is the amount of herbicide required to inhibit 80% of growth relative to that of the untreated control. Values are determined by visual inspection of stand reduction and fresh weight of the samples. These herbicides were also applied postemergence on 14-day-old plants grown as described above at rates ranging from 0.004 to 5.6 kg ha⁻¹. Pans were maintained in the greenhouse, and herbicidal activity was determined as described in the preemergence section.

Cellular Leakage. Cellular damage was measured by detection of electrolyte leakage into the bathing medium with an electrical conductivity meter designed for assaying 1 mL of bathing medium and returning it to the Petri dish (Kenyon et al., 1985). Conductivity was monitored for 14 h of continuous light after a 20 h incubation in darkness. Because of difference in background conductivity between treatment solutions, results were expressed as change in electrical conductivity after initial measurement at the beginning of the light period (these compounds did not induce leakage in the

dark). All treatments for electrolyte leakage measurements were triplicated.

Porphyrin Determination. All extractions for HPLC determinations of Proto IX were made under dim, green light after 20 h of incubation in 10 μM technical grade isoxazole solutions in darkness at 25 °C. Samples (approximately 0.1 g of barley leaf disks) were homogenized in 2 mL of HPLC grade methanol/0.1 N NH₄OH (9:1 v/v) with a Brinkman Polytron at full speed for 15 s. The homogenate was washed four times with 2 mL of hexane and centrifuged (6000g, 10 min, 4 °C). The supernatants were filtered through a 0.2 μm nylon syringe filter. Samples were stored in light-tight, aluminum foil-wrapped, glass vials at –20 °C until analyzed by HPLC.

The HPLC system consisted of the following Waters Associates components: Model 510 pump, a Model 712 autosampler, a Maxima 820 controller, and Models 470 fluorescence and 990 photodiode spectrophotometric detectors. The column was a 250 × 4.6 mm (i.d.) Spherisorb 5 μm ODS-1 reversed-phase column preceded by a Bio-Rad ODS-5S guard column. The solvent system was 70% HPLC grade methanol with 30% PIC A reagent, and the injection volume was 50 μL. The position of Proto IX in samples was determined by injecting Proto IX standard. Proto IX was detected with the fluorescence detector using excitation and emission wavelengths at 400 and 630 nm, respectively. The data were expressed on a molar basis per gram of fresh weight. All treatments were triplicated.

Protox Assay. Crude etioplasts were prepared for *in vitro* experiments as before (Lee et al., 1993). All procedures were conducted under dim, green light source. Leaves of dark-grown barley seedlings were cut into small pieces and homogenized with a Sorvall Omni-Mixer twice for 30 s at full speed using a fresh weight/volume ratio of 1:3. Homogenization buffer consisted of 50 mM *N*-2-hydroxyethylpiperazine-*N*-2-ethanesulfonic acid (HEPES, pH 7.8), 330 mM sucrose, 1 mM MgCl₂, 1 mM ethylenediaminetetraacetic acid (EDTA), and 2.5 mM dithiothreitol (DTT). The homogenate was filtered through one layer of Miracloth and then centrifuged (200g, 5 min, 4 °C) to remove crude cell debris. The resulting supernatant was centrifuged (1500g, 20 min, 4 °C). The pelleted crude etioplasts were resuspended in a suspension buffer using a small paintbrush. The suspension buffer was composed of 50 mM HEPES (pH 7.8) and 330 mM sucrose. The etioplasts were stored at –80 °C until use.

Before Protox assay, the extracts of etioplasts were thawed and sonicated twice for 5 s at 0 °C. Protein concentration was determined according to the method of Bradford (1976), and the extracts were adjusted to 4 mg of protein mL⁻¹ in the suspension buffer. Each compound (Table 1) was added in a volume of 30 μL of methanol or acetone to 300 μL of the extract. Equivalent volumes of methanol or acetone were added to control treatments. The extracts were incubated on ice for 10 min with or without the test compound prior to assay.

Protogen was prepared according to the procedure of Jacobs and Jacobs (1982) with the following modifications. Proto IX stock solution (0.5 mM in 20% ethanol containing 10 mM KOH) was reduced to Protogen with approximately one-eighth volume of freshly ground sodium amalgam. The resulting colorless solution was adjusted to pH 8.0 by addition of an equal volume of (5× strength) assay buffer, consisting of 500 mM HEPES (pH 7.5) and 25 mM EDTA, and filtered through a 0.2 μm nylon syringe filter. DTT was added to the Protogen solution in a light-tight glass to a final concentration of 100 mM. The resulting preparation was stable in dim, green light at room temperature for at least 2 h.

Protox was assayed according to the procedure of Sherman et al. (1991a) with the following modifications. The assay mixture consisted of 100 mM HEPES (pH 7.5) and 5 mM EDTA. Protox activity was determined under saturated substrate conditions (2 mM Protogen) in the presence of 0–100 μM technical grade herbicide. The reaction was initiated by addition of 0.1 mL of extract with or without the test compounds to 0.9 mL of assay mixture and monitored for 90 s at 30 °C. Fluorescence was monitored directly from the assay mixture using a Shimadzu RF-5000U, temperature-controlled, recording spectrofluorometer with excitation and emission wavelengths set at 395 and 622 nm, respectively. The reaction

rate was essentially constant over a 2 min period. Autoxidation of Protogen to Proto IX in the presence of heat-inactivated (80 °C for 15 min) extract was negligible. All treatments for Protox assays were duplicated and repeated in time.

Binding Studies. Binding of [¹⁴C]acifluorfen (AF) to barley etioplasts in the presence or absence of test compounds was determined according to the method of Tischer and Strotmann (1977). Etioplasts (0.6 mg of protein) were suspended in a 1 mL reaction solution consisting of 330 mM sorbitol, 100 mM HEPES (pH 7.7), 1 mM EDTA, and 1 mM MgCl₂. Various concentrations (2–100 nM) of ¹⁴C-labeled AF (specific activity of 18.03 mCi mmol⁻¹, uniformly ring labeled) plus 100 nM of the nonlabeled technical grade test compounds were added. The suspensions were thoroughly mixed and incubated for 30 min on ice. The samples were centrifuged (6 min, 12000g, 4 °C). The supernatant was transferred to vials and mixed with 12 mL of premixed scintillation cocktail (Ecolume) for radioactivity measurements. The inner walls of tubes were dried with cotton swabs without disturbing the pellets to remove excess [¹⁴C]AF. A 100 μL aliquot of tissue solubilizer (Protosol) was added to the pellets and heated in a water bath at 50 °C for 15 min. The slurry was neutralized with 50 μL of 1 M tris-(hydroxymethyl)aminomethane hydrochloride (Tris-HCl) and transferred to vials. Ethanol (50 μL) used to wash the inner walls of each tube was combined with the slurry before radioactivity measurements. The amount of bound [¹⁴C]AF was calculated from the radioactivity in the pellets. Specific binding constants were estimated from double-reciprocal plots of bound AF vs free AF (Tischer and Strotmann, 1977). For example, extrapolation of the regression lines of [¹⁴C]AF binding to the *x*-axis (shown in Figure 3A) gave a value of 0.04831 1/nM or 20.7 nM, which is the specific binding constant of AF.

Estimation of Partition Coefficients. Reversed-phase high-performance liquid chromatography (RP-HPLC) was used for the determination of octanol/water partition coefficients (*P*) of herbicides (Ellgenhausen et al., 1981). The RP-HPLC technique involved determination of capacity factors (*k'*) for a set of standard compounds with a wide range of known experimental partition coefficients. The *k'* values were calculated from

$$k' = (t_r - t_0)/t_0 \quad (1)$$

where *t_r* is the retention time of the compound and *t₀* is the retention time of the nonsorbed standard compound (acetone). A standard curve of log *P* versus *k'* was constructed. Using the same RP-HPLC conditions as in the standard curve, the capacity factors for the herbicides were determined. The log *P* for the herbicides was calculated using the linear regression equation of the form

$$\log P = a + b(\log k') \quad (2)$$

The RP-HPLC system was composed of the same Waters Associates components that were used for the Proto IX determination. The mobile phase was methanol/water (75:25), and the flow rate was 1.4 mL min⁻¹. The injection volume was 5 μL. The detector was set at 254 nm. Three replicate determinations were made for each compound.

Molecular Properties. The molecular properties of isoxazoles were calculated using Chem-X (Chemical Design Limited, Chipping Norton, Oxfordshire, U.K., January 1995 version) molecular modeling software and procedures as described in our previous work (Nandihalli et al., 1992a,b). Compound **1** was selected as a molecular template upon which the molecular properties of the other isoxazoles were fitted because it had relatively high Protox-inhibiting activity. The three-dimensional chemical structure of compound **1** was built using standard atoms and fragments available in the molecular mechanics parameter library of the Chem-X software. The low-energy form of the structure was obtained using molecular mechanics optimization. The structure was subjected to full geometry optimization via MOPAC (Quantum Chemistry Program Exchange 560, version 6.0, Department of Chemistry, Indiana University, Bloomington, Indiana) using AM1 (Austin

Table 2. Herbicidal Activity of 10 Isoxazole Compounds Applied Pre- and Postemergence

compd	preemergent GR ₈₀			postemergent GR ₈₀		
	MG	VL	BG	MG	VL	BG
1	6.4	0.56	>5.6	>11.2	>11.2	>11.2
2	0.86	0.18	1.12	5.6	6.4	9.0
3	>11.2	>11.2	>11.2	>11.2	>11.2	>11.2
4	5.6	4.7	9.0	6.4	11.2	>11.2
5	0.164	0.064	0.167	0.151	0.202	2.46
6	0.46	0.071	0.23	0.062	0.071	1.12
7	0.060	0.004	0.060	0.009	0.005	0.18
8	2.2	0.28	0.25	0.11	0.20	0.90
9	0.071	0.062	0.22	0.20	0.071	0.18
10	0.28	3.0	0.46	5.9	0.62	3.5

^a Herbicidal activity is expressed as a GR₈₀ (kg ha⁻¹), which is the amount of herbicide required to inhibit 80% of weed growth relative to that of an untreated control. MG, morningglory; VL, velvetleaf; BG, barnyardgrass.

Model) parametrization. Structures of the other isoxazoles in the study were derived from the optimized structure of compound **1**. These structures were also optimized for geometry as above. Each optimized isoxazole was fitted to the optimized structure of compound **1** before its molecular properties were calculated. The structures of two Protox inhibitors, acifluorfen and RH-1422, and the Protogen were also built and optimized as described above before their molecular properties were generated.

RESULTS AND DISCUSSION

In Vivo Effects of Isoxazoles. At the whole plant level, the acid and methyl ester derivatives (**1–4**) had better preemergence than postemergence activity but were, as a group, relatively less active than the other isoxazoles studied (Table 2). The carboxylic acid derivative (**3**) had no herbicidal activity regardless of the application method (Table 2). The acid chloride derivative (**4**) was relatively more active than the carboxylic acid derivative but did not perform as well as the methyl ester derivatives (**1** and **2**). These isoxazoles caused little injury to the leaf disks, inducing <20% of potential leakage after 14 h of light exposure (Figure 1).

The carboxamide series (**5–7**) was very active against the weeds studied. These compounds provided excellent preemergence weed control at rates as low as 4 g ha⁻¹ (Table 2). The addition of a propargyl substituent in the 5-position yielded the most active isoxazole (**7**) in both whole plants and in the leaf disk assay (Figure 1). This compound induced photobleaching of the leaf disks 8 h after light exposure. The other amides were less phytotoxic (Figure 1) and did not cause bleaching of the tissues during the 14 h exposure to light.

The amino acid series consisted of *R* and *S* enantiomers applied individually or in a mixture (**8–10**). The *R* enantiomer was generally more active than the *S* enantiomer in whole plants (Table 2) and leaf disk assay (Figure 1). The activity of the enantiomer mixture was, in most cases, between those of the enantiomers applied individually. The *R* enantiomer induced the second to the highest leakage (Figure 1) and caused photobleaching 14 h after light exposure. The enantiomer mixture induced the third highest phytotoxic response in the leaf disk assay, the activity probably deriving from the presence of the *R* component.

All of the isoxazoles, except for the carboxylic acid derivative, had higher herbicidal activity when applied preemergence than postemergence. This is in contrast with most Protox-inhibiting herbicides that usually have better postemergence activity than preemergence. However, other Protox-inhibiting molecules, such as certain

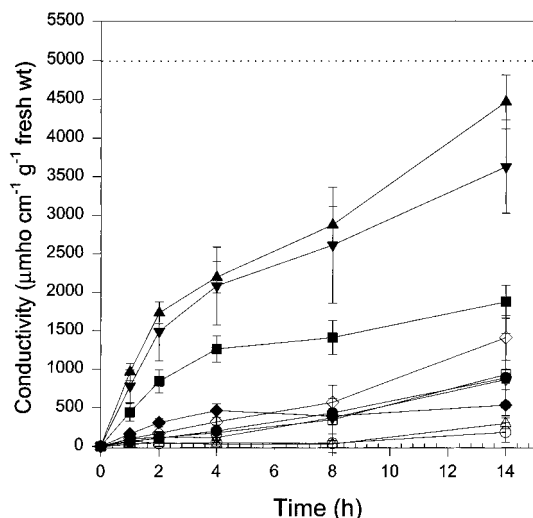


Figure 1. Herbicidal activity of the isoxazole herbicides as measured by electrolyte leakage from damaged cells. Barley leaf disks were incubated in the presence of 10 μM of each test compound for 20 h in darkness and then exposed to continuous light. Time 0 represents the beginning of light exposure: (○) 1; (□) 2; (△) 3; (▽) 4; (◇) 5; (●) 6; (▲) 7; (■) 8; (▼) 9; (◆) 10; (dotted line) maximum conductivity obtained 24 h after samples were boiled. No leakage was observed in the control treatment. Data are the means of three measurements \pm SD.

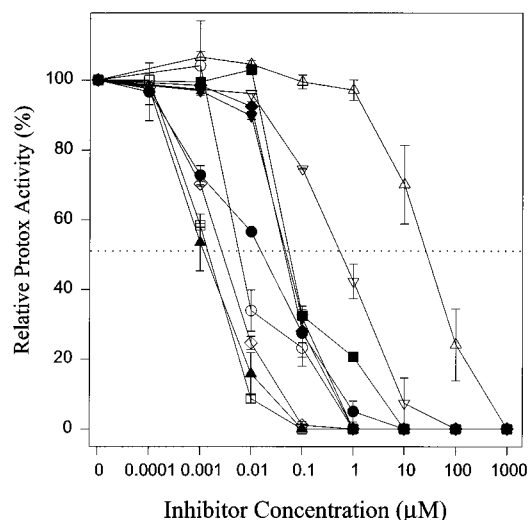


Figure 2. Effect of the isoxazole herbicides on Protox activity of soybean etioplasts measured under initial velocity conditions: (○) 1; (□) 2; (△) 3; (▽) 4; (◇) 5; (●) 6; (▲) 7; (■) 8; (▼) 9; (◆) 10; (dotted line) 50% inhibition of activity. Data are the means of three measurements \pm SD.

phenyltriazolinones (Dayan et al., 1996) and substituted uracils (Wright et al., 1995), also have excellent premergence activity.

In Vitro Effects of Isoxazoles. Despite their relatively low *in vivo* activities, the methyl ester and acid chloride derivatives (1, 2, 4) were potent inhibitors of Protox (Figure 2), and their binding affinity to the enzyme (Figure 3) correlated well with their Protox I_{50} values (Figure 4). However, they induced relatively low levels of Proto IX accumulation (Table 3). The carboxylic acid derivative did not compete for the AF binding site on the enzyme (Figure 3A) and was a poor Protox inhibitor (Figure 2). The levels of Proto IX in the carboxylic acid-treated tissues were similar to those in untreated plants.

Since resistance to Protox inhibitors can be achieved by the metabolic degradation of the herbicides (Frear

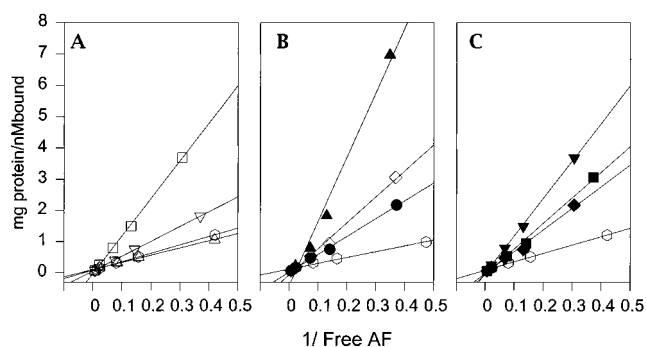


Figure 3. Binding of labeled acifluorfen (AF) in the presence of 100 nM unlabeled isoxazole compounds. Carboxylic acid and methyl ester series (A): (+) AF alone; (□) 2; (△) 3; (▽) 4. Carboxamide series (B): (+) AF alone; (◇) 5; (●) 6; (▲) 7. Amino acid series (C): (+) AF alone; (■) 8; (▼) 9; (◆) 10. Data are the means of three measurements.

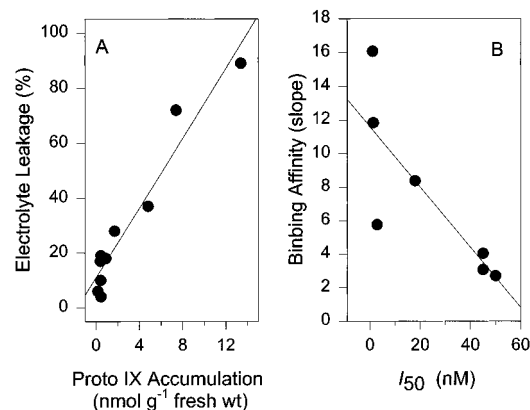


Figure 4. Relationship between Proto IX accumulation and electrolyte leakage (A) and I_{50} values and binding affinities (B) of the compounds.

Table 3. Biological Activities of Isoxazoles

compd	Protox I_{50} , nM	Proto IX, ^a nmol g ⁻¹ fresh wt	leakage, ^b % of max	log P
1	6	0.45 \pm 0.03	4	4.2446
2	1.3	0.46 \pm 0.02	19	4.2775
3	25000	0.17 \pm 0.05	6	
4	550	0.40 \pm nd	17	4.2536
5	2.8	1.17 \pm 0.11	28	2.4251
6	18	0.89 \pm 0.07	18	2.5991
7	1.1	13.38 \pm 1.97	89	2.3045
8	50.0	4.78 \pm 0.16	37	
9	45	7.38 \pm 0.30	72	2.9158
10	45	0.43 \pm 0.04	10	3.2081
control		0.17 \pm 0.03		

^a Proto IX levels were measured at 20 h after dark incubation in the presence of 10 μM test compound. ^b Leakage values are calculated from conductivity of bathing solution at 14 h after light exposure.

et al., 1983; Dayan et al., 1996), it may also be a factor involved in the contrast between the relatively lower *in vivo* herbicidal activity of the methyl ester (1 and 2) and acid chloride (4) derivatives and their ability to inhibit Protox. Indeed, hydrolysis of the methyl ester bond on the carbonyl moiety on the 4-position of the isoxazole ring would yield biologically inactive carboxylic acid derivatives. The short incubation period at low temperature required for the Protox assay and the binding study precluded any significant degradation of the compounds, permitting the unaltered observation of the interaction between the compounds and the molecular target site. Under these conditions, the methyl ester and acid chloride derivatives exhibited

Table 4. Molecular Properties of Isoxazoles

parameter ^a	compd									
	1	2	3	4	5	6	7	9	10	
μ , D	0.999	2.779	2.385	1.848	4.364	4.27	5.929	5.36	5.159	
TEI, eV	204.5	179.3	166.9	157.3	169.9	168.8	215.6	252.4	252.5	
α , A ³	21.3	20.8	19.5	19.9	19.8	20.2	24.7	26.9	26.9	
ϵ_{HOMO} , eV	-10.49	-9.97	-9.79	-9.92	-9.96	-10	-9.85	-10.2	-10.16	
ϵ_{LUMO} , eV	-1.582	-1.406	-1.528	-1.608	-1.235	-1.268	-1.341	-1.316	-1.292	
S_{HOMO} , eV	-0.191	-0.204	-0.204	-0.202	-0.201	-0.2	-0.203	-0.196	-1.197	
S_{LUMO} , eV	-1.264	-1.423	-1.309	-1.244	-1.619	-1.577	-1.492	-1.519	-1.547	
S_{E} , eV	-6.679	-5.198	-5.537	-5.536	-5.592	-5.631	-6.998	-8.17	-8.177	
S_{N} , eV	-28	2.6	-0.2	172.5	13.6	22.3	32.5	6.5	-5.1	
VDW _{volume} , A ³	213	207	195	203	195	207	243	276	278	
VDW _{area} , A ²	200	191	171	186	177	181	217	256	256	
-MEP _{volume} , A ³	118	137	107	80	138	152	220	201	206	
-MEP _{area} , A ²	144	137	115	93	137	153	194	206	209	
+MEP _{volume} , A ³	138	92	83	74	116	102	125	138	131	
+MEP _{area} , A ²	155	117	112	98	134	128	160	1267	164	

^a μ , dipole moment; TEI, total electrostatic interaction; α , molecular polarizability; ϵ_{HOMO} , energy of highest occupied molecular orbital; ϵ_{LUMO} , energy of lowest unoccupied molecular orbital; S_{HOMO} and S_{LUMO} , superdelocalizability of highest occupied and lowest unoccupied molecular orbitals, respectively; S_{E} , electrophilic superdelocalizability; S_{N} , nucleophilic superdelocalizability; VDW_{volume} and VDW_{area}, van der Waals volume and area, respectively; -MEP_{volume} and -MEP_{area}, negative molecular electrostatic potential volume and area, respectively; +MEP_{volume} and +MEP_{area}, positive molecular electrostatic potential volume and area, respectively.

strong competitive binding to Protox. However, plant deesterases could conceivably degrade these derivatives into biologically inactive carboxylic forms during the more prolonged exposure of the whole plant study and the leaf disk assay.

All of the carboxamide derivatives (5–7) were potent Protox inhibitors (Figure 2). Compound 7 was the strongest Protox inhibitor with an I_{50} of 1.1 nM (Table 3) and had the highest binding affinity to the enzyme (Figure 3C). The inhibition of Protox activity by the other amides was less than that by the propargyl derivative (Figure 2) and commensurate to their respective binding to the enzyme (Figure 3C). The propargyl derivative (7) induced the highest level of Proto IX accumulation of all the isoxazole herbicides tested.

The enantiomers, individually or in a mixture, had similar *in vitro* inhibition of Protox (Table 3), in spite of the differences observed among their activities at the whole plant level. However, the herbicidal activity of these compounds correlated well with their ability to induce Proto IX to accumulate, i.e. the *R* enantiomer induced greater Proto IX accumulation than the *S* enantiomer (Table 3). Nandihalli et al. (1994) have shown that *R* enantiomers of diphenyl ether and pyrazole phenyl ether herbicides were consistently more active than the *S* enantiomers. However, the *in vivo* activity of these compounds correlated with their *in vitro* activities.

In our particular case, the *in vivo* activity of the enantiomers was different from their ability to inhibit Protox; therefore, factors other than stereoselective inhibition of Protox may be involved. We have shown that the carboxylic acid derivative of the methyl ester series was biologically inactive. Plants have many deesterases that could also be involved in the hydrolytic cleavage of the ethyl moiety on the amino group. This carboxylic acid metabolite may be more or less active than the ester parent. Since plant deesterases are typically stereospecific, the difference in *in vivo* activity between the two enantiomers could be associated with a differential rate of metabolism between the *R* and *S* derivatives.

There were correlations between *in vivo* parameters ($r^2 = 0.93$), i.e. the level of Proto IX accumulation and the cellular damage induced by the compounds (Figure 4A), as well as between *in vitro* parameters ($r^2 = 0.66$),

i.e. the I_{50} values and the binding affinities of the compounds (Figure 4B). However, there was no clear relationship between the *in vivo* and *in vitro* activities, indicating that factors other than Protox inhibition (e.g. metabolism) modulate the phytotoxicity of this series of compounds. Similar observations have been reported with other Protox-inhibiting compounds (Nandihalli et al., 1992a; Reddy et al., 1995).

Molecular Properties. The bulk, electronic, and energy parameters of nine isoxazole compounds studied are presented in Table 4. There were large differences in molecular properties such as dipole moment, total electrostatic interaction, molecular polarizability, various superdelocalizabilities, and volumes among the compounds (Table 4). The more active Protox inhibitors (7 and 9) had higher dipole moments, molecular polarizabilities (related to lipophilicity), total electrostatic interactions, van der Waals areas (VDW_{area}), van der Waals volumes (VDW_{volume}), and positive and negative molecular electrostatic potential areas and volumes (+MEP_{area}, +MEP_{volume}, -MEP_{area}, -MEP_{volume}) than the least active compound (3). Compound 1 was inactive, although the values of some of its molecular properties (VDW_{area}, VDW_{volume}, +MEP_{area}, and +MEP_{volume}) were similar to those of the active compound 7. This may be partly due to differences in electronic and energy parameters observed between the two compounds.

The *R* enantiomer (9) of isoxazole is more active than the *S* enantiomer (10). The bulk (VDW_{area} and VDW_{volume}), energy (energy of highest occupied molecular orbital, ϵ_{HOMO} , and energy of lowest unoccupied molecular orbital, ϵ_{LUMO}), and various electronic properties were not significantly different (Table 4). Calculated S_{N} and dipole moments were higher in the *R* than in the *S* enantiomer; however, these properties will be identical if determined experimentally. The optimized structures of the chiral pairs differ with respect to spatial arrangement mainly around the chiral center. Since both enantiomers inhibit Protox equally, differences in herbicidal activity are not likely to be due to chiral specificity at the enzyme level. Other factors such as metabolism (discussed earlier) may play more significant roles.

Pearson correlation analysis of all the molecular properties of nine isoxazoles (Table 4) revealed that

Table 5. Bulk, Electronic, and Energy Properties of Protogen and Active and Inactive Protox Inhibitors

property ^a	compd				
	Protogen	acifluorfen	RH-1422	7	3
Protox I_{50} , nM		20	21	1	25000
bulk descriptors					
x -axis, Å	10.6	9.0	10.1	10.5	10.5
y -axis, Å	11.6	8.2	8.4	8.7	5.5
VDW _{area} , Å ²	404	205	213	217	171
VDW _{volume} , Å ³	439	224	237	243	195
electronic descriptors					
dipole moment, D	5.580	4.894	5.651	5.929	2.385
molecular polarizability, Å ³	50.8	23.5	24.0	24.7	19.6
S_N , eV	75.94	89.23	21.89	32.25	-0.18
S_E , eV	-13.268	-6.830	-7.009	-6.998	-5.537
-MEP _{volume} , Å ³	470	226	294	220	107
energy descriptors					
TEI, eV	472.4	221.8	225.6	214.6	166.8
MOPAC _{electronic} , eV	-72346	-31745	-28744	-31935	-22503
MOPAC _{nuclear} , eV	65334	26221	24243	26474	18143

^a For abbreviated descriptor terms, refer to Table 4.

dipole moment was most significantly correlated with log Proto IX ($r = 0.74$) and log conductivity ($r = 0.78$). However, the simple regression equation based on the dipole moment did not account for variation (differences between observed and predicted) >55% in log Proto IX and 60% in log conductivity. Multiple regression analysis revealed that the molecular polarizability (α), electrophilic superdelocalizability (S_E), and +MEP_{volume} descriptors were related to log Proto IX and log conductivity. The relevant regression equations are given below.

$$\log \text{Proto IX} = -5.0099 + 0.7179\alpha + 2.1304S_E + 0.0253(+\text{MEP}_{\text{volume}}) \quad (3)$$

$$F_{(3,5)} = 5.87; \quad s = 0.37; \quad r^2 = 0.78$$

$$\log \text{conductivity} = -0.6009 + 0.6181\alpha + 1.7546S_E + 0.0105(+\text{MEP}_{\text{volume}}) \quad (4)$$

$$F_{(3,5)} = 5.25; \quad s = 0.28; \quad r^2 = 0.76$$

In these equations Proto IX accumulation and cellular leakage were positively related to the lipophilicity and +MEP_{volume} of the molecule and negatively related to the electrophilic superdelocalizability. The equations for isoxazoles differ from the equations we have reported for other compounds (Nandihalli et al., 1992a,b; Reddy et al., 1995). While Proto IX accumulation and electrical conductivity were related to electronic properties of the isoxazole compounds, these biological activities were related to electronic as well as bulk, energy, and log P descriptors for various other Protox inhibitors previously studied.

Protox inhibitors are known to act as competitive inhibitors of the enzyme Protox by binding to the same active sites as the substrate Protogen (Varsano et al., 1990; Camadro et al., 1991; Matringe et al., 1992; Nandihalli et al., 1992a). To examine this, we have attempted to compare the chemical similarities between Protogen and the most active compound (Table 5). To broaden the comparison, we have also included the least active compound (**3**) as well as two known Protox inhibitors of different chemical groups, acifluorfen (Matringe et al., 1989b; Witkoski and Halling, 1989; Duke et al., 1991) and RH-1422 (Nandihalli et al., 1992b). The x - and y -axes of Cartesian coordinates of these molecules reveal that all have similar x -axes but

differ in their y -axes. The three active compounds had similar y -axis values, which were higher than the least active compound (Table 5). The dipole moment of three active compounds is similar to that of Protogen. The VDW_{area} and VDW_{volume}, which depict the overall size and shape of the molecule, suggested that the active compounds had about half of the volume and area of Protogen molecule (Table 5). The bulk descriptors of the least active compound were smaller than those of the active molecules. Furthermore, α , S_E , total electrostatic interaction, electronic and nuclear energies, and -MEP_{volume} of three active compounds are similar and are approximately half of the Protogen molecule (Table 5).

The distribution of positive and negative molecular electrostatic potentials calculated from atomic point charges is shown in Figure 5. The -MEP on the molecule indicates the region most likely involved in the initial interaction with an approaching electrophile (Nandihalli et al., 1992a). The -MEP in Protogen is distributed in six distinct regions, four on pyrrole rings and two on propionate side chains (Figure 5). It should be mentioned that we corrected an error that had been made in previous construction of the optimized Protogen molecule. Protogen has two propionate side chains and has six distinct -MEP regions; the earlier structure was constructed with two propyl groups and only had four -MEP regions (Nandihalli et al., 1992a,b).

In acifluorfen, a larger -MEP region is located in the vicinity of the NO₂-COOH region and in RH-1422, two larger -MEP regions are located on CO₂-isopropyl and on the oxygen bridge. The -MEP distributions in the most active (**7**) and least active (**3**) isoxazole were somewhat similar on two rings, but the -MEP on the CONH₂ region was larger for the active than for the least active compound. Furthermore, compound **7** had an additional -MEP region at the propargyl region. We believe that these larger -MEP regions of the active compounds mimic the reactive part of the Protogen molecule and apparently are involved in enzyme binding processes.

Conclusions. We have demonstrated that a group of isoxazoles are herbicidal due to inhibition of Protox. Certain isoxazoles had some of the lowest I_{50} values to have been reported so far. However, *in vitro* activity of the compounds did not always correlate well with their *in vivo* activity. This is particularly evident with the methyl ester series that strongly inhibited Protox activity but had relatively low herbicidal activity. We believe

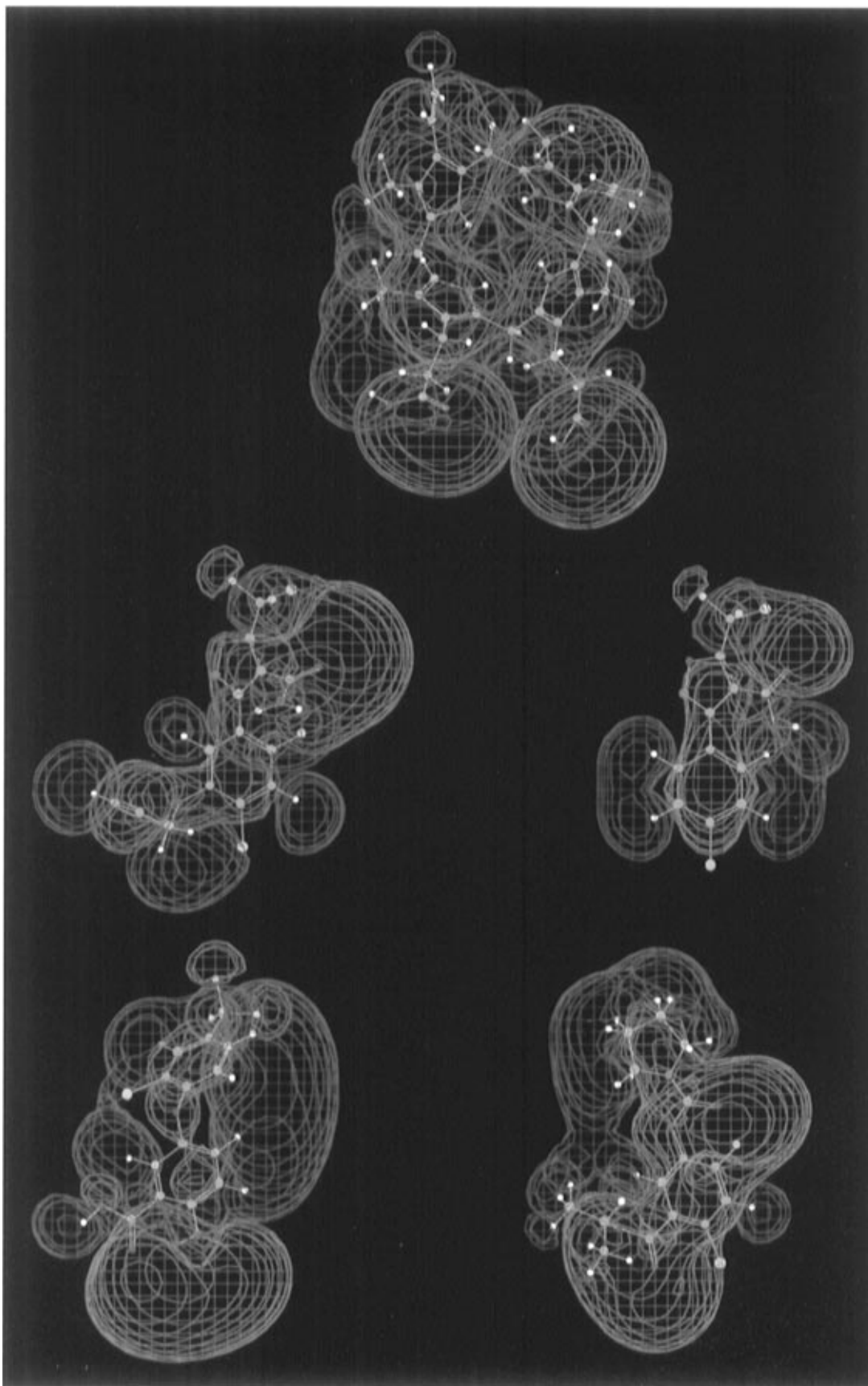


Figure 5. Molecular electrostatic potential (MEP) distribution (± 10 kcal/mol) of (A, top) Protogen, (B, middle left) active isoxazole (7), (C, middle right) inactive isoxazole (3), (D, bottom left) acifluorfen, and (E, bottom right) RH-1422. Blue regions = negative MEP; red regions = positive MEP.

that these derivatives may be rapidly hydrolyzed to form metabolically inactive carboxylic acid derivatives. The herbicidal activity of these compounds was better

estimated by determining the amount of Proto IX they caused to accumulate *in vivo*.

The bulk, electronic, and energy properties of the most

active Protox inhibitors of different chemistry are similar and closely approximated half of the Protopogen molecule. The difference in herbicidal activity between *R* and *S* enantiomers of an isoxazole was not seen at the Protox level, indicating that spatial arrangement of the chiral center might differently affect metabolic degradation of the herbicide.

LITERATURE CITED

- Beale, C.; Weinstein, J. D. Tetrapyrrole metabolism in photosynthetic organisms. *Biosynthesis of Hemes and Chlorophylls*; Dailey, H. A., Ed.; McGraw-Hill Book: New York, 1990; pp 287–391.
- Becerril, J. M.; Duke, S. O. Acifluorfen effects on intermediates of chlorophyll synthesis in green cucumber cotyledon tissues. *Pestic. Biochem. Physiol.* **1989a**, *35*, 119–126.
- Becerril, J. M.; Duke, S. O. Protoporphyrin IX content correlates well with activity of photobleaching herbicides. *Plant Physiol.* **1989b**, *90*, 1175–1181.
- Camadro, J.-M.; Matringe, M.; Scalla, R.; Labbe, P. Kinetic studies on protoporphyrinogen oxidase inhibition by diphenyl ether herbicides. *Biochem. J.* **1991**, *277*, 17–21.
- Dayan, F. E.; Weete, J. D.; Hancock, H. G. Physiological basis for differential sensitivity to sulfentrazone by sicklepod (*Senna obtusifolia*) and coffee senna (*Cassia occidentalis*). *Weed Sci.* **1996**, *44*, 12–17.
- Duke, S. O.; Kenyon, W. H. Peroxidizing activity determined by cellular leakage. In *Target Assays for Modern Herbicides and Related Phytotoxic Compounds*; Böger, P., Sandmann, G., Eds.; Lewis: Boca Raton, FL, 1993; pp 61–66.
- Duke, S. O.; Becerril, J. M.; Sherman, T. D.; Lydon, J.; Matsumoto, H. The role of protoporphyrin IX in the mechanism of action of diphenyl ether herbicides. *Pestic. Sci.* **1990**, *30*, 367–378.
- Duke, S. O.; Lydon, J.; Becerril, J. M.; Sherman, T. D.; Lehnen, L. P.; Matsumoto, H. Protoporphyrinogen oxidase-inhibiting herbicides. *Weed Sci.* **1991**, *39*, 465–473.
- Duke, S. O.; Nandihalli, U. B.; Lee, H. J.; Duke, M. V. Protoporphyrinogen oxidase as the optimal herbicide site in the porphyrin pathway. *Am. Chem. Soc. Symp. Ser.* **1994**, *No. 559*, 191–204.
- Ellgenhausen, H.; D'Hondt, C.; Fuerer, R. Reversed-phase chromatography as a general method for determining octanol/water partition coefficients. *Pestic. Sci.* **1981**, *12*, 219–227.
- Frear, D. S.; Swanson, H. R.; Mansager, E. R. Acifluorfen metabolism in soybean: diphenylether bond cleavage and the formation of homoglutathione, cysteine and glucose conjugates. *Pestic. Biochem. Physiol.* **1983**, *20*, 299–310.
- Hamper, B. C.; Leschinsky, K. L.; Massey, S. S.; Bell, C. L.; Brannigan, L. H.; Prosch, S. D. Synthesis and herbicidal activity of 3-aryl-5-(haloalkyl)-4-isoxazolecarboxamides and their derivatives. *J. Agric. Food Chem.* **1995**, *43*, 219–228.
- Jacobs, N. J.; Jacobs, J. M. Assay for enzymatic protoporphyrinogen oxidation, a late step in heme biosynthesis. *Enzyme* **1982**, *28*, 206–219.
- Jacobs, J. M.; Jacobs, N. J. Oxidation of protoporphyrinogen to protoporphyrin, a step in chlorophyll and haem synthesis. *Biochem. J.* **1987**, *244*, 219–224.
- Jacobs, J. M.; Jacobs, N. J. Protoporphyrin accumulation and export by isolated barley (*Hordeum vulgare* L.) plastids: effects of diphenyl ether herbicides. *Plant Physiol.* **1993**, *101*, 1181–1188.
- Jacobs, J. M.; Jacobs, N. J.; Sherman, T. D.; Duke, S. O. Effect of diphenyl ether herbicides on oxidation of protoporphyrinogen to protoporphyrin in organellar and plasma membrane enriched fractions of barley. *Plant Physiol.* **1991**, *97*, 197–203.
- Kenyon, W. H.; Duke, S. O.; Vaughn, K. C. Sequences of effects of acifluorfen on physiological and ultrastructural parameters in cucumber cotyledon discs. *Pestic. Biochem. Physiol.* **1985**, *24*, 240–250.
- Kojima, S.; Matsumoto, H.; Ishizuka, K. Protoporphyrin IX accumulation in *Lemna paucicostata* Hegelm. caused by diphenyl ether herbicides and their herbicidal activity. *Weed Res.* **1991**, *36*, 318–323.
- Lee, H. J.; Duke, S. O. Protoporphyrinogen IX-oxidizing activities involved in the mode of action of peroxidizing herbicides. *J. Agric. Food Chem.* **1994**, *42*, 2610–2618.
- Lee, H. J.; Duke, M. V.; Duke, S. O. Cellular localization of protoporphyrinogen-oxidizing activities of etiolated barley (*Hordeum vulgare* L.) leaves. *Plant Physiol.* **1993**, *102*, 881–889.
- Lee, H. J.; Duke, M. V.; Birk, J. H.; Yamamoto, M.; Duke, S. O. Biochemical and physiological effects of benzheterocycles and related compounds. *J. Agric. Food Chem.* **1995**, *43*, 2722–2727.
- Matringe, M.; Scalla, R. Photoreceptors and respiratory electron flow involvement in the achlorophyllous soybean cells. *Pestic. Biochem. Physiol.* **1987**, *27*, 267–274.
- Matringe, M.; Scalla, R. Effects of acifluorfen-methyl on cucumber cotyledons: porphyrin accumulation. *Pestic. Biochem. Physiol.* **1988**, *40*, 128–132.
- Matringe, M.; Camadro, J.-M.; Labbe, P.; Scalla, R. Protoporphyrinogen oxidase inhibition by three peroxidizing herbicides: oxadiazon, LS 82-556 and M&B 39279. *FEBS Lett.* **1989a**, *245*, 35–38.
- Matringe, M.; Camadro, J.-M.; Labbe, P.; Scalla, R. Protoporphyrinogen oxidase as a molecular target for diphenyl ether herbicides. *Biochem. J.* **1989b**, *260*, 231–235.
- Matringe, M.; Mornet, R.; Scalla, R. Characterization of [³H]-acifluorfen binding to purified pea etioplasts, and evidence that protoporphyrinogen oxidase specifically binds acifluorfen. *Eur. J. Biochem.* **1992**, *209*, 861–868.
- Matsumoto, H.; Duke, S. O. Acifluorfen-methyl effects on porphyrin synthesis in *Lemna paucicostata* Hegelm. *J. Agric. Food Chem.* **1990**, *38*, 2066–2071.
- Nandihalli, U. B.; Duke, S. O. The porphyrin pathway as a herbicide target site. *Am. Chem. Soc. Symp. Ser.* **1993**, *No. 524*, 62–78.
- Nandihalli, U. B.; Duke, M. V.; Duke, S. O. Quantitative structure-activity relationships of protoporphyrinogen oxidase-inhibiting diphenyl ether herbicides. *Pestic. Biochem. Physiol.* **1992a**, *43*, 193–211.
- Nandihalli, U. B.; Duke, M. V.; Duke, S. O. Relationships between molecular properties and biological activities of *O*-phenyl pyrrolidino- and piperidinocarbamate herbicides. *J. Agric. Food Chem.* **1992b**, *40*, 1993–2000.
- Nandihalli, U. B.; Duke, M. V.; Ashmore, J. W.; Musco, V. A.; Clark, R. D.; Duke, S. O. Enantioselectivity of protoporphyrinogen oxidase-inhibiting herbicides. *Pestic. Sci.* **1994**, *40*, 265–277.
- Reddy, K. N.; Nandihalli, U. B.; Lee, H. J.; Duke, M. V.; Duke, S. O. Predicting activity of protoporphyrinogen oxidase inhibitors by computer-aided molecular modeling. In *Protoporphyrinogen Oxidase Inhibitors*; American Chemical Society: Washington, DC, 1995; pp 211–224.
- Scalla, R.; Matringe, M. Inhibitors of protoporphyrinogen oxidase as herbicides: diphenyl ethers and related photobleaching herbicides. *Rev. Weed Sci.* **1994**, *6*, 103–132.
- Scalla, R.; Matringe, M.; Camadro, J.-M.; Labbe, P. Recent advances in the mode of action of diphenyl ether and related herbicides. *Z. Naturforsch.* **1990**, *45C*, 503–511.
- Sherman, T. D.; Becerril, J. M.; Matsumoto, H.; Duke, M. V.; Jacobs, J. M.; Jacobs, N. J.; Duke, S. O. Physiological basis for differential sensitivities of plant species to protoporphyrinogen oxidase-inhibiting herbicides. *Plant Physiol.* **1991a**, *97*, 280–287.
- Sherman, T. D.; Duke, M. V.; Clark, R. D.; Sanders, E. F.; Matsumoto, H.; Duke, S. O. Pyrazole phenyl ether herbicides inhibit protoporphyrinogen oxidase. *Pestic. Biochem. Physiol.* **1991b**, *40*, 236–245.
- Tischer, W.; Strotmann, H. Relationship between inhibitor binding by chloroplasts and inhibition of photosynthetic electron transport. *Biochim. Biophys. Acta* **1977**, *460*, 113–125.
- Varsano, R.; Matringe, M.; Magnin, N.; Mornet, R.; Scalla, R. Competitive interaction of three peroxidizing herbicides with the binding of [³H]acifluorfen to corn etioplast membranes. *FEBS Lett.* **1990**, *272*, 106–108.

- Watanabe, H.; Ohori, Y.; Sandmann, G.; Wakabayashi, K.; Böger, P. Quantitative correlation between short-term accumulation of protoporphyrin IX and peroxidative activity of cyclic imides. *Pestic. Biochem. Physiol.* **1992**, *42*, 99–109.
- Witkoski, D. A.; Halling, B. P. Inhibition of plant protoporphyrinogen oxidase by the herbicide acifluorfen-methyl. *Plant Physiol.* **1989**, *90*, 1239–1242.
- Wright, T. R.; Fuerst, E. P.; Ogg, A. G.; Nandihalli, U. B.; Lee, H. J. Herbicidal activity of UCC-C4243 and acifluorfen is due to inhibition of protoporphyrinogen oxidase. *Weed Sci.* **1995**, *43*, 47–54.

Received for review September 13, 1996. Accepted November 6, 1996.®

JF9607019

® Abstract published in *Advance ACS Abstracts*, February 1, 1997.